Available online at www.sciencedirect.com
ScienceDirect
Biochimica et Biophysica Acta 1783 (2008) 874–885
Biochimica et Biophysica Acta BBA
www.elsevier.com/locate/bbamcr

Store-operated Ca^{2+} channels and Stromal Interaction Molecule 1 (STIM1) are targets for the actions of bile acids on liver cells

Edoardo C. Aromataris [a,1], Joel Castro [b,1], Grigori Y. Rychkov [a], Greg J. Barritt [b,*]

[a] School of Molecular and Biomedical Science, University of Adelaide, Adelaide, South Australia, 5005, Australia
[b] Department of Medical Biochemistry, School of Medicine, Flinders University, GPO Box 2100, Adelaide SA 5001, Australia

Received 16 August 2007; received in revised form 7 February 2008; accepted 11 February 2008
Available online 23 February 2008

Abstract

Cholestasis is a significant contributor to liver pathology and can lead to primary sclerosis and liver failure. Cholestatic bile acids induce apoptosis and necrosis in hepatocytes but these effects can be partially alleviated by the pharmacological application of choleretic bile acids. These actions of bile acids on hepatocytes require changes in the release of Ca^{2+} from intracellular stores and in Ca^{2+} entry. However, the nature of the Ca^{2+} entry pathway affected is not known. We show here using whole cell patch clamp experiments with H4-IIE liver cells that taurodeoxycholic acid (TDCA) and other choleretic bile acids reversibly activate an inwardly-rectifying current with characteristics similar to those of store-operated Ca^{2+} channels (SOCs), while lithocholic acid (LCA) and other cholestatic bile acids inhibit SOCs. The activation of Ca^{2+} entry was observed upon direct addition of the bile acid to the incubation medium, whereas the inhibition of SOCs required a 12 h pre-incubation. In cells loaded with fura-2, choleretic bile acids activated a Gd^{3+}-inhibitable Ca^{2+} entry, while cholestatic bile acids inhibited the release of Ca^{2+} from intracellular stores and Ca^{2+} entry induced by 2,5-di-(*tert*-butyl)-1,4-benzohydro-quinone (DBHQ). TDCA and LCA each caused a reversible redistribution of stromal interaction molecule 1 (STIM1, the endoplasmic reticulum Ca^{2+} sensor required for the activation of Ca^{2+} release-activated Ca^{2+} channels and some other SOCs) to puncta, similar to that induced by thapsigargin. Knockdown of STIM1 using siRNA caused substantial inhibition of Ca^{2+}-entry activated by choleretic bile acids. It is concluded that choleretic and cholestatic bile acids activate and inhibit, respectively, the previously well-characterised Ca^{2+}-selective hepatocyte SOCs through mechanisms which involve the bile acid-induced redistribution of STIM1.

Keywords: Liver cell; Cholestasis; Ca^{2+} channel; STIM1; Bile acid; Patch clamp recording

1. Introduction

Cholestasis arises from hepatocyte dysfunction, or intrahepatic or extrahepatic biliary obstruction, leading to impaired secretion of bile into the bile canaliculus and impaired movement of bile along the biliary tree. Causes of cholestasis include primary sclerosing cholangitis, primary biliary cirrhosis, liver injury, and genetic abnormalities in hepatocyte bile acid transporters. If untreated cholestasis can ultimately progress to liver failure (reviewed in [1–3]). Cholestasis is associated with decreases in the expression and/or activity of hepatocyte bile acid transporters, and the accumulation of conjugated and unconjugated bile acids in hepatocytes and the blood [4]. The more hydrophobic bile acids, including taurolithocholic (TLCA), lithocholic (LCA), cholic (CA) and taurocholic (TCA) acids, inhibit bile flow (are cholestatic), while the less hydrophobic bile acids, including taurodeoxycholic (TDCA), tauroursodeoxycholic (TUDCA) and ursodeoxycholic (UDCA) acids, enhance bile blow (are choleretic) [2]. TLCA is a potent inducer of cholestasis [5,6], and cholestatic bile acids induce liver injury leading to apoptosis and necrosis of hepatocytes [7–12]. The choleretic bile acids TUDCA and UDCA have been used at pharmacological doses to treat cholestasis [13–23].

Central to the actions of bile acids on hepatocytes are bile acid-induced changes in the cytoplasmic free Ca^{2+} concentration ($[Ca^{2+}]_{cyt}$) resulting from the release of Ca^{2+} from the endoplasmic reticulum (ER), and/or the activation of Ca^{2+} entry. In hepatocytes 7and liver cell lines many bile acids increase $[Ca^{2+}]_{cyt}$,

* Corresponding author. Tel.: +61 8 8204 4260; fax: +61 8 8374 0139.
E-mail address: Greg.Barritt@flinders.edu.au (G.J. Barritt).
[1] Each author contributed equally to the work.

0167-4889/$ - see front matter © 2008 Elsevier B.V. All rights reserved.
doi:10.1016/j.bbamcr.2008.02.011

release Ca^{2+} from intracellular stores, and induce Ca^{2+} entry, while TLCA inhibits Ca^{2+} entry [24–30]. TUDCA may enhance bile flow by activating Ca^{2+} entry and increasing hepatocyte $[Ca^{2+}]_{cyt}$ [26,27,29,30]. This, in turn, may activate Ca^{2+}-dependent myosin light chain kinase and the polymerisation of F-actin, and enhance contraction of the bile canaliculus [31]. While the effects of bile acids on the release of Ca^{2+} from intracellular stores in hepatocytes [25,26] and other cell types [32] have been reasonably well described, little is known about the Ca^{2+} entry pathways modulated by bile acids.

The main Ca^{2+} entry pathway activated by hormones and growth factors in hepatocytes is the store-operated Ca^{2+} channel (SOC) [33–36]. While only one type of SOC has been detected in hepatocytes and in hepatocyte cell lines [33,34], several other types of Ca^{2+} entry channels are known to be present, although most have not been well-characterised [37]. There is some evidence to indicate that Ca^{2+} entry through SOCs is required for the maintenance of normal bile flow [38]. Hepatocyte SOCs exhibit a high selectivity for Ca^{2+} and electrophysiological properties essentially indistinguishable from those of Ca^{2+} release-activated Ca^{2+} channels in mast cells and lymphocytes [34,36]. Under physiological conditions, SOCs are activated by a decrease in the Ca^{2+} concentration in the ER induced by the actions of IP_3 and Ca^{2+} on IP_3 receptors (reviewed in [39]). SOCs can also be activated pharmacologically by inhibiting the ER ($Ca^{2+}+Mg^{2+}$) ATP-ase (SERCA) (reviewed in [39]).

Recent studies with other cell types have shown that Orai (CRACM) proteins constitute the pore of Ca^{2+}-selective SOCs, while stromal interaction molecule (STIM) proteins constitute the Ca^{2+} sensor which detects the decrease in Ca^{2+} in the ER and conveys this information to Orai1 in the plasma membrane (reviewed in [40–42]). The release of Ca^{2+} from the ER alters the localisation of STIM1 in the ER, and in some studies STIM1 has been observed to move to locations adjacent to the plasma membrane, the junctional ER [43–49]. STIM1 redistribution is necessary for SOC activation in lymphocytes, mast cells, some other cell types (reviewed in [41,42]) and liver cells [50].

The aim of the present experiments was to identify the Ca^{2+} entry channel(s) involved in the actions of choleretic and cholestatic bile acids on hepatocyte $[Ca^{2+}]_{cyt}$. The experiments have been conducted with the H4-IIE rat liver cell line and with isolated rat hepatocytes. The results indicate that the main type of hepatocyte plasma membrane Ca^{2+} entry channel activated by choleretic bile acids and inhibited by cholestatic bile acids is the hepatocyte Ca^{2+}-selective SOC, and provide evidence that bile acids affect SOCs by modifying the intracellular localisation of STIM1. SOCs and STIM1 may provide a potential target for pharmacological interventions in the treatment of cholestasis and cholestasis-induced liver damage.

2. Materials and methods

2.1. Materials

Collagenase (Type IV) was obtained from Worthington Biochemical Corporation; Dulbecco's Modified Eagles Medium (DMEM), fura-2 (acetoxymethylester), goat anti-mouse Alexa-Fluor 488 antibody and pluronic acid F-127 from Invitrogen Australia, Mt Waverley, Victoria; D-myo-inositol 1, 4, 5-trisphosphate (IP_3), ionomycin, bile acids, and 2-aminoethyl diphenylborate (2-APB) from Sigma Australia; thapsigargin and 2,5-di-(*tert*-butyl)-1,4-benzohydro-quinone (DBHQ) from Sapphire Bioscience; mouse anti-GOK STIM1 monoclonal antibody from BD Biosciences Pharmingen, San Jose, CA, USA; FuGENE 6 from Roche Pharmaceutical, Nutley, NJ, USA; the pDsRed2-ER plasmid from Clontech, Mountain View, CA, USA; and glass coverslips from Menzel-Glaser GmgH, Braunschweig, Germany. The GFP-STIM1 plasmid, in which cDNA encoding GFP is located immediately downstream of the predicted signal sequence of the STIM1 gene and inserted into the pApuro expression vector (GFP-STIM1/pApuro) [43] was kindly provided by Dr T Kurosaki, RIKEN Research Centre for Allergy and Immunology, Kanagwa, Japan.

2.2. Cell culture

H4-IIE rat liver cells (ATCC CRL 1548) [51] were plated on No. 1 glass coverslips, (12, 22 and 30 mm diameter for immunofluorescence, fura-2 and live cell confocal imaging experiments, respectively) and cultured for 24–72 h in DMEM supplemented with 10% (v/v) fetal calf serum, penicillin (100 U/ml), streptomycin (0.1 mg/ml) and 10 mM HEPES in 5% (v/v) CO_2 (pH 7.4) at 37 °C, as described previously [33,34]. Hepatocytes were isolated from rat liver by perfusion with collagenase, as described previously [35]. Animals received humane care, and the experimental protocols were conducted according to the criteria outlined in the "Australian Code of Practice for the Care and Use of Animals for Scientific Purposes" (National Health and Medical Research Council of Australia). Hepatocytes were plated on glass coverslips pre-treated with concentrated HCl to facilitate their attachment, then cultured for 24–72 h in DMEM/F12 supplemented with 10% (v/v) fetal calf serum, penicillin/streptomycin and HEPES in 5% (v/v) CO_2 (pH 7.4) at 37 °C.

2.3. Electrophysiology

Whole-cell patch clamping was performed at room temperature using a computer-based patch clamp amplifier (EPC-9 HEKA Electronics, Germany) and PULSE software (HEKA Electronics) [35]. The bath solution contained (mM): NaCl, 140; CsCl, 4; $CaCl_2$, 10; $MgCl_2$, 2; glucose, 10; and HEPES, 10; adjusted to pH 7.4 with NaOH. The internal solution contained (mM): Cs glutamate, 120; $CaCl_2$, 5; $MgCl_2$, 5; MgATP, 1; EGTA, 10; and HEPES, 10; adjusted to pH 7.2 with NaOH. Depletion of the intracellular Ca^{2+} stores was achieved by addition of 20 μM IP_3 to the internal solution. Patch pipettes were pulled from borosilicate glass and fire-polished; pipette resistance ranged between 2 and 4 MΩ. In order to monitor the development of the SOC current (I_{SOC}), voltage ramps between −138 and +102 mV were applied every 2 s, starting immediately after achieving the whole cell configuration. All voltages shown have been corrected for the liquid junction potential of −18 mV between the bath and electrode solutions (estimated by JPCalc [52]). The holding potential was −18 mV throughout. Cell capacitance was compensated automatically by the EPC9 amplifier.

2.4. Measurements of $[Ca^{2+}]_{cyt}$ using fura-2

Cells attached to glass coverslips were incubated with 5 μM fura-2 acetoxymethylester in Krebs–Ringer–HEPES buffer containing 0.02% (v/v) pluronic acid. The Krebs–Ringer–HEPES solution contained (mM): NaCl, 136; KCl, 4.7; $CaCl_2$, 1.3; $MgCl_2$, 1.25; glucose, 10; and HEPES, 10; adjusted to pH 7.4 with NaOH. Isolated hepatocytes were loaded for 1 h at 37 °C, while H4-IIE cells were loaded for 30 min at room temperature. Fura-2 fluorescence was measured at room temperature in cells incubated in Krebs–Ringer–HEPES in the presence of the indicated concentrations of $CaCl_2$, using a Nikon TE300 Eclipse microscope in conjunction with a Sutter DG-4/OF wavelength switcher, Omega XF04 filter set for fura-2, Photonic Science ISIS-3 ICCD camera and UIC Metafluor software. Fluorescence images at 340 nm and 380 nm excitation were obtained every 20 s using a 40× objective.

Values of fluorescence ratio (340 nm:380 nm) were converted to $[Ca]_{cyt}$ using the equation and K_d value derived by Grynkiewicz et al. [53] for the binding of fura-2 to Ca^{2+}, and ionomycin and EGTA to determine the maximum (R_{max}) and minimum (R_{min}) ratios. The results are expressed as means±SEM (between 10 and 20 cells for each experiment). Initial rates of Ca^{2+} entry were

determined using a Ca^{2+} "add-back" protocol in which cells were initially incubated in the absence of extracellular Ca^{2+} (Ca^{2+}_{ext}), treated with agonist to activate the Ca^{2+} entry pathway, then Ca^{2+}_{ext} was added (1.3, 2.4 or 10 mM as indicated in the figures and text), and the increase in $[Ca^{2+}]_{cyt}$ was measured as a function of time. The initial rate of increase in $[Ca^{2+}]_{cyt}$ was determined by linear regression. Values for the peak (maximum) $[Ca^{2+}]_{cyt}$ observed after Ca^{2+}_{ext} addition were determined by calculating the difference between the maximum $[Ca^{2+}]_{cyt}$ observed after Ca^{2+}_{ext} re-addition and the value of $[Ca^{2+}]_{cyt}$ obtained immediately before Ca^{2+}_{ext} re-addition. Amounts of Ca^{2+} released were determined by measuring the height of the peak of the DBHQ- or bile acid-induced increase in $[Ca^{2+}]_{cyt}$.

2.5. Cell transfection, immunofluorescence, and fluorescence microscopy

H4-IIE cells were transfected with GFP-STIM1/pApuro or pDsRed2-ER DNA (3 μg) or co-transfected with both plasmids using FuGENE 6, according to the manufacturer's instructions. The cells were then incubated at 37 °C for 48–72 h before imaging GFP (488 nm excitation/500–550 nm emission) or pDsRed2 (561 nm excitation/550–620 nm emission) fluorescence using a Leica SP5 scanning confocal microscope. For the measurement of STIM1 by immunofluorescence, H4-IIE cells (attached to glass coverslips) were washed 3 times with phosphate buffered saline (PBS) and then fixed in 3% (v/v) paraformaldehyde at room temperature for 10 min. The fixed cells were washed 5 times with 100 mM glycine in PBS and permeabilised with 0.1% (v/v) saponin in PBS for 10 min at room temperature. Cells were washed 5 times in PBS, then blocked with blocking buffer (gelatin 0.2% (w/v) plus TWEEN 0.1% (w/v) in PBS) for 30 min at room temperature, incubated with mouse anti-GKO/STIM1 (1:100 dilution in blocking buffer) for 3 h, and washed 5 times with blocking buffer. The cells were then incubated with Alexa-Fluor 488-conjugated goat anti-mouse IgG (1:500 dilution in blocking buffer) for 1 h, washed 5 times with PBS and the coverslips mounted on slides in IMMU-Mount medium (Thermo Shandon, Pittsburgh, PA, USA). Fluorescence was imaged by confocal microscopy (488 nm excitation/500–550 nm emission).

2.6. Transfection of cells with siRNA targeted against STIM1

The sequences of siRNA targeted against STIM1 and control siRNA and cell transfection were as described by Litjens et al. [50].

2.7. Statistical analysis

Statistical significance was assessed using Student's *t*-test to compare two samples. Multiple groups were compared using ANOVA followed by the Bonferroni *post hoc* test. Differences between means were considered significant at $P \leq 0.05$. Curves showing activation of the I_{SOC} under different conditions were compared using 2-way ANOVA.

3. Results

3.1. Choleretic bile acids activate Ca^{2+} entry through SOCs in H4-IIE liver cells and rat hepatocytes

To test whether bile acids can affect membrane conductance, whole cell patch clamping experiments were conducted with H4-IIE liver cells. When applied to the bath at concentrations between 100 and 300 μM, the choleretic bile acids TDCA, TUDCA and UDCA each activated an inwardly-rectifying membrane current (Fig. 1A and B). The activation was reversible as shown by the observation that the current induced by UDCA was completely inactivated within 3–4 min upon washout of the bile acid (Fig. 1C). When IP_3 was included in the pipette solution to deplete intracellular Ca^{2+} stores and activate I_{SOC}, the subsequent application of choleretic bile acids had no effect on

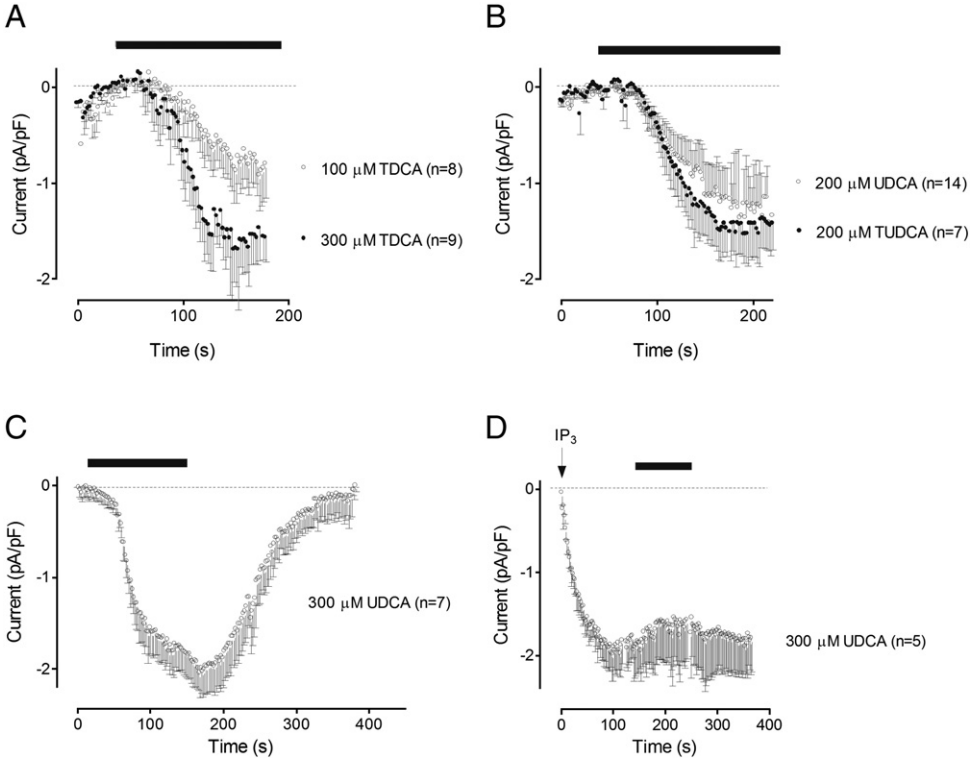

Fig. 1. Choleretic bile acids activate a Ca^{2+} current in H4-IIE liver cells with properties similar to those of I_{SOC}. (A, B) Inward currents measured at −118 mV in the presence of TDCA, UDCA and TUDCA plotted against time. The horizontal bar shows the time of the addition of a bile acid to the bath. The internal solution did not contain IP_3. (C) The effect of UDCA is reversible. (D) UDCA does not activate further current over and above that activated by IP_3. The results are the means ± SEM of the number of experiments indicated.

membrane conductance (shown for UDCA in Fig. 1D), indicating that choleretic bile acids and IP_3 activate the same current.

The *I–V* plot of the current activated by choleretic bile salts showed marked inward rectification and a reversal potential above 100 mV (Fig. 2A). The current recorded in response to voltage steps negative to −100 mV showed fast inactivation, similar to that of the I_{SOC} previously characterised in H4-IIE cells and rat hepatocytes (Fig. 2B). This current could be blocked by 1 μM La^{3+} and was abolished by the replacement of the extracellular Ca^{2+} by Mg^{2+} (not shown). To confirm that the current activated by choleretic bile acids is the hepatocyte I_{SOC}, medium containing 100 mM Ba^{2+} in place of 10 mM Ca^{2+} was applied to the bath after the current induced by TUDCA had developed. This produced a spike in the amplitude of the inward current followed by inhibition (Fig. 2C), characteristic of the properties of I_{SOC} in H4-IIE cells [33,34]. Furthermore, current activated by choleretic bile acids was inhibited by 2-APB (Fig. 2D). Unlike choleretic bile acids, the cholestatic bile acids (LCA and TLCA) did not activate I_{SOC} in H4-IIE cells when applied to the bath at similar concentrations (100–300 μM) (results not shown).

To test whether the activation of Ca^{2+} entry through SOCs by choleretic bile acids is associated with the release of Ca^{2+} from intracellular stores and an increase in $[Ca^{2+}]_{cyt}$, changes in $[Ca^{2+}]_{cyt}$ were measured using fura-2. When added to H4-IIE cells incubated in the presence of 2.4 mM Ca^{2+}_{ext}, TDCA (300 μM) caused a substantial increase in $[Ca^{2+}]_{cyt}$ (Fig. 3A). Further experiments on bile acid-induced activation of Ca^{2+} entry were conducted at 10 mM Ca^{2+}_{ext}, the same concentration of Ca^{2+}_{ext} as that employed in the patch clamping experiments. At 10 mM Ca^{2+}_{ext}, TDCA-induced an increase in $[Ca^{2+}]_{cyt}$ similar to that observed at 2.4 mM Ca^{2+}_{ext} (Fig. 3B). In the presence of TDCA, $[Ca^{2+}]_{cyt}$ decreased to the basal level when $[Ca^{2+}]_{ext}$ was reduced from 10 mM to zero (Fig. 3B). The ability of TDCA to increase $[Ca^{2+}]_{cyt}$ is retained when Ca^{2+}_{ext} and TDCA are washed out and then re-introduced to the perfusion medium (Fig. 3B). The TDCA-induced increase in $[Ca^{2+}]_{cyt}$ was substantially reduced to near basal values by addition of Gd^{3+} (10 μM) (Fig. 3C). To confirm that TDCA induces Ca^{2+} release from intracellular stores under conditions employed to measure Ca^{2+} entry, cells were incubated in the presence of 2.4 mM Ca^{2+}_{ext} and 10 μM Gd^{3+} (to block Ca^{2+} entry). Addition of TDCA caused a transient increase in Ca^{2+}_{cyt} (Fig. 3D) indicating the release of Ca^{2+} from intracellular stores. No TDCA-induced release of Ca^{2+} from intracellular stores was observed when the bile acid was added in the absence of extracellular Ca^{2+} (results not shown). The reason for this is not clear, however. It may be because extracellular Ca^{2+} affects the solubility of bile acids and their ability to form micelles [54,55].

In cells incubated in the presence of 10 mM Ca^{2+}_{ext}, the addition of TDCA following thapsigargin did not cause a further increase in $[Ca^{2+}]_{cyt}$ (Fig. 4A). The magnitude of the plateau following TDCA addition was similar to that following thapsigargin addition (Fig. 4B *cf* A and C). These results provide further evidence that TDCA activates the same Ca^{2+} entry pathway as that activated by SERCA inhibitors.

The choleretic bile acid TUDCA (300 μM) also caused an increase in $[Ca^{2+}]_{cyt}$ (Fig. 5). Consistent with previous observations [26] the TUDCA-induced increase in $[Ca^{2+}]_{cyt}$ was observed as oscillations in $[Ca^{2+}]_{cyt}$. The oscillatory increases in $[Ca^{2+}]_{cyt}$ were dependent on $[Ca^{2+}]_{ext}$ and were substantially reduced by addition of Gd^{3+} (Fig. 5), indicating a requirement for Ca^{2+} entry through SOCs in the maintenance of Ca^{2+}_{cyt} oscillations.

The effects of bile acids on Ca^{2+} entry in rat hepatocytes were also investigated. When added directly to the hepatocyte incubation medium, TDCA increased $[Ca^{2+}]_{cyt}$ in the presence of 10 mM Ca^{2+}_{ext} (Fig. 3E). This increase was inhibited by 10 μM Gd^{3+} (results not shown).

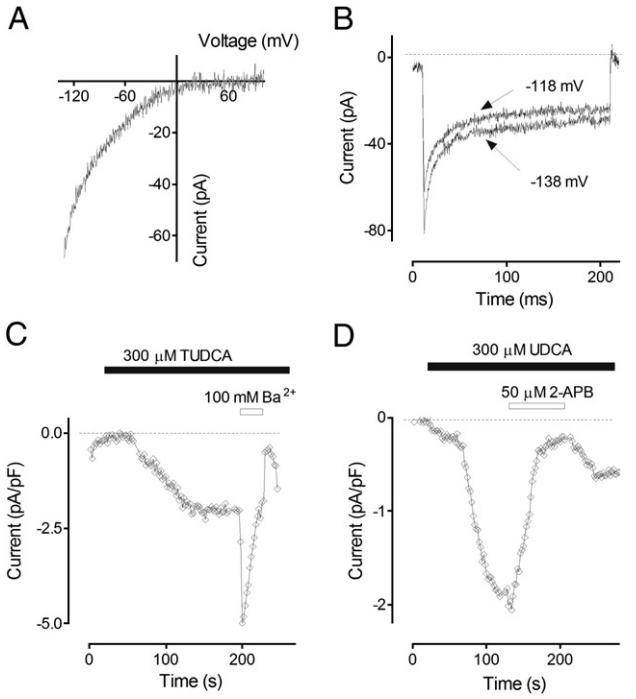

Fig. 2. Properties of the current activated by choleretic bile acids. (A) I–V plot and (B) current traces in response to −118 and −138 mV steps obtained for cells incubated in the presence of 300 μM TDCA. (C) The effect of substitution of Ba^{2+} for Ca^{2+} in the extracellular medium on the current induced by TUDCA. The horizontal bars show the time of addition of TUDCA and of the application of an extracellular medium composed of an iso-osmolar solution containing 100 mM Ba^{2+} in place of the medium containing 10 mM Ca^{2+}. (D) Inhibition of the current induced by UDCA by 2-APB (50 μM). The horizontal bars show the times of addition of UDCA and 2-APB. The results are representative of those obtained from 5 to 7 cells.

3.2. Cholestatic bile acids inhibit Ca^{2+} entry through SOCs in H4-IIE cells and rat hepatocytes

To test whether bile acids inhibit Ca^{2+}-entry through SOCs in H4-IIE liver cells, whole cell patch clamping experiments were performed using IP_3 (20 μM in the patch pipette) to induce I_{SOC} [34,36] (Fig. 6A, control curve). The IP_3-initiated current was inhibited by the cholestatic bile acids DCA (~25% inhibition), CA (~40%), TLCA (~40%) and LCA (~80%) at a concentration of 50 μM, when these were pre-incubated with H4-IIE cells for 12 h before the measurement of I_{SOC} (examples of TLCA and LCA are shown in Fig. 6A). When tested at

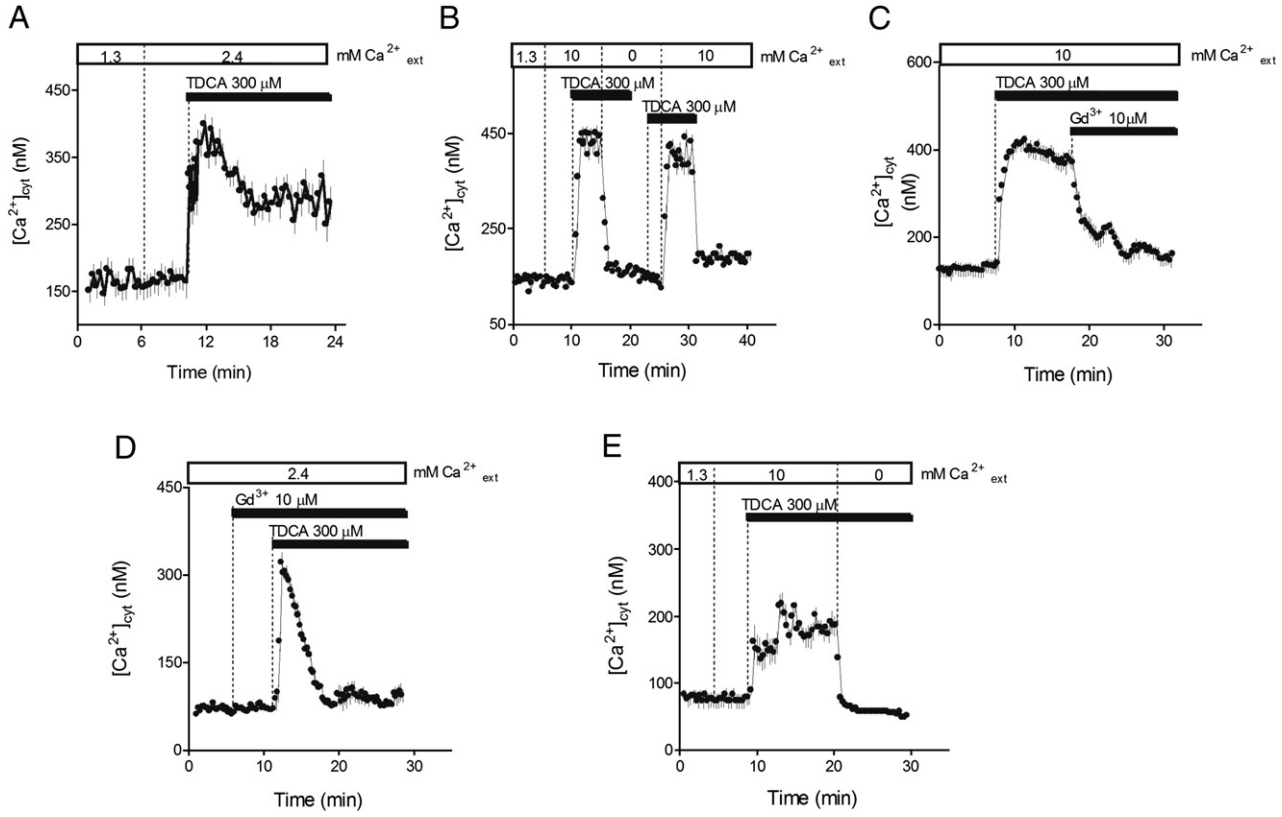

Fig. 3. The choleretic bile acid TDCA reversibly activates Ca^{2+} entry, measured using fura-2, in H4-IIE liver cells and in rat hepatocytes. (A) TDCA induces an increase in $[Ca^{2+}]_{cyt}$ in the presence of 2.4 mM Ca^{2+}_{ext}. (B) The TDCA-induced increase in $[Ca^{2+}]_{cyt}$ at 10 mM Ca^{2+}_{ext}, is abolished when $[Ca^{2+}]_{ext}$ is reduced to zero in the presence of TDCA. A second addition of TDCA increases $[Ca^{2+}]_{cyt}$ in the presence of 10 mM $[Ca^{2+}]_{ext}$. This increase in $[Ca^{2+}]_{cyt}$ is abolished when TDCA is removed from the extracellular medium (in the presence of 10 mM Ca^{2+}_{ext}). (C) The increase in $[Ca^{2+}]_{cyt}$ induced by TDCA is inhibited by 10 μM Gd^{3+}. (D) In the presence of 2.4 mM Ca^{2+}_{ext} and 10 μM Gd^{3+} (to inhibit Ca^{2+} entry), TDCA induces a transient increase in $[Ca^{2+}]_{cyt}$ indicating Ca^{2+} release from intracellular stores. (E) TDCA reversibly activates Ca^{2+} entry in rat hepatocytes. The measurement of $[Ca^{2+}]_{cyt}$ as a function of time in cells loaded with fura-2 was conducted as described in Materials and methods. The additions to the bath are indicated by the horizontal bars. The results shown are representative of those obtained for one of 3 or more experiments which each gave similar results.

10 μM, CA, LCA and TLCA each inhibited the current by 25, 27 and 20%, respectively (result for LCA shown in Fig. 6A). Two-way ANOVA showed that at 10 μM concentration the effect of these bile acids on the development of I_{SOC} was significant ($P<0.001$). No inhibition of I_{SOC} was observed when the cholestatic bile acid was added directly to the bath (results not shown). Unconjugated forms of LCA and CA caused greater inhibition than their conjugated counterparts (TLCA and TCA, respectively), possibly due to the greater hydrophobicity of the unconjugated forms. DCA and TCA (50 μM) had little effect on I_{SOC} (not shown). In similar experiments in which cells were incubated for 12 h with a choleretic

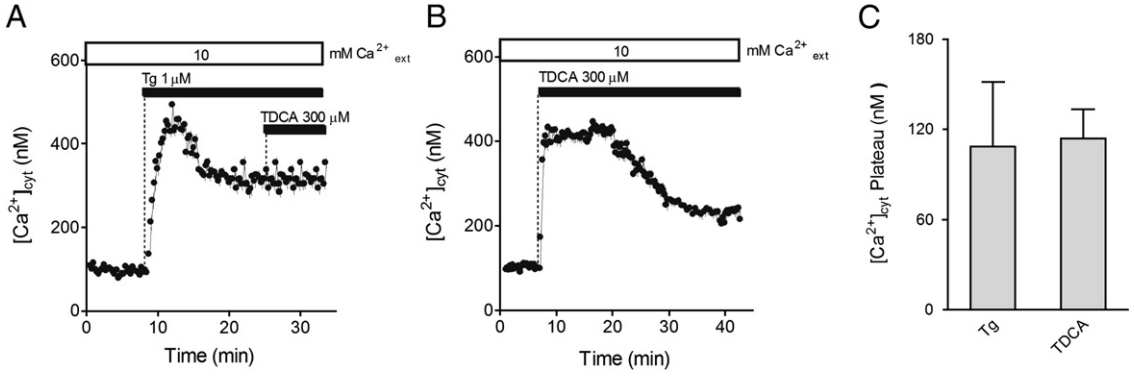

Fig. 4. The effects of TDCA and thapsigargin are not additive. (A) Effect of addition of TDCA following thapsigargin. (B) Effect of addition of TDCA. (C) The magnitude of the plateaus following TDCA or thapsigargin addition. $[Ca^{2+}]_{cyt}$ was measured as a function of time in H4-IIE cells loaded with fura-2, as described in Materials and methods. The additions to the bath are indicated by the horizontal bars. The results shown in (A) and (B) are representative of those obtained for one of 3 experiments which each gave similar results. The values in (C) are the means ± SEM of 3 experiments ($P>0.05$).

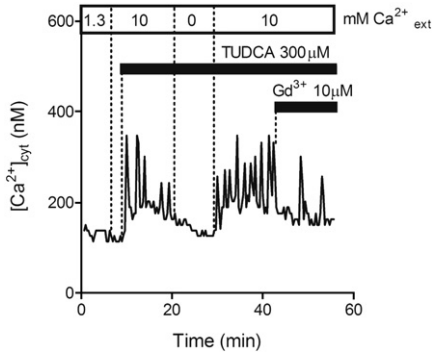

Fig. 5. TUDCA activates Ca^{2+} entry associated with oscillations in $[Ca^{2+}]_{cyt}$ in H4-IIE liver cells. $[Ca^{2+}]_{cyt}$ was measured as a function of time in H4-IIE cells loaded with fura-2, as described in Materials and methods. The additions to the bath are indicated by the horizontal bars. The results shown are representative of those obtained for one of 3 experiments which each gave similar results.

bile acid (50 μM of TDCA, TUDCA or UDCA), no inhibition of the IP_3-initiated current was observed (Fig. 6B).

Of all cholestatic bile salts tested, LCA (50 μM) had the strongest inhibitory effect (~80%) on the amplitude of I_{SOC} activated by intracellular IP_3. However, when I_{SOC} was activated by application of 300 μM of UDCA to the bath, LCA had much weaker inhibitory effect, reducing the current by ~50% (Fig. 6C). In cells treated with LCA (50 μM) the I_{SOC} activated by UDCA was approximately twice as large ($P<0.001$, 2-way ANOVA) than that activated by IP_3 (Fig. 6C (LCA) *cf* Fig. 6A (IP_3)). These results indicate that the choleretic bile acid UDCA can counteract the inhibitory effects of cholestatic bile acids on Ca^{2+} entry through SOCs.

To test the effects of cholestatic bile acids on the release of Ca^{2+} from intracellular stores and Ca^{2+} entry monitored by measuring changes in $[Ca^{2+}]_{cyt}$, experiments were conducted with cells loaded with fura-2. Pre-incubation of H4-IIE cells with LCA (50 μM) for 12 h greatly reduced the ability of DBHQ to induce the release of Ca^{2+} from intracellular stores, and inhibited Ca^{2+} entry (Fig. 7A, B and C). When the bile acid was added directly to the incubation medium immediately before measuring changes in $[Ca^{2+}]_{cyt}$ there was no effect on DBHQ-induced Ca^{2+} release or Ca^{2+} entry (results not shown). Pre-incubation for 12 h with CA (50 μM) also caused a decrease in DBHQ-induced Ca^{2+} release and Ca^{2+} entry (Fig. 7A, B and C). These results confirm, using fura-2, that cholestatic bile acids inhibit Ca^{2+} entry through SOCs, and indicate that pre-incubation with LCA or CA leads to a release of Ca^{2+} in intracellular stores. When the choleretic bile acid TDCA was added to cells pre-incubated for 12 h with the cholestatic bile acid LCA, a substantial increase in $[Ca^{2+}]_{cyt}$ was observed (Fig. 7D), suggesting that TDCA can counteract the inhibition of Ca^{2+} entry caused by pre-incubation with a cholestatic bile acid.

In rat hepatocytes, cholestatic bile acids also inhibited Ca^{2+} entry when pre-incubated with the cells for 12 h. LCA and CA (50 μM) each inhibited both the initial rate and plateau of the increase in $[Ca^{2+}]_{cyt}$ induced by the addition of 1.3 mM Ca^{2+}_{ext} to hepatocytes previously incubated in the absence of added Ca^{2+}_{ext} and in the presence of DBHQ (results not shown). The initial rates of Ca^{2+} entry were 121±11, 21±3.3 and 33±7.2 nM/min and the values of the plateau reached after Ca^{2+}_{ext} addition were 120±18, 51±8.2 and 70±2.4 nM for control, LCA, and CA, respectively (means±SEM for 3–4 experiments). (The degrees of significance, determined using ANOVA followed by the Bonferroni *post hoc* test, were $P<0.01$ for comparison of the initial rate for the control with each of the initial rates for LCA and CA, and $P<0.05$ for comparison of the value of the plateau for the control with that of the plateau for LCA.) These decreases in the rate and plateau of Ca^{2+} entry were associated with a substantial reduction in the DBHQ-induced release of Ca^{2+} from intracellular stores (results not shown). The amount of Ca^{2+} released was 39±7, 3.9±1.2 and 13.8±6.9 nM for control, LCA and CA, respectively. (The degrees of significance (ANOVA followed by the Bonferroni *post hoc* test) were $P<0.01$ and $P<0.05$ for comparison of the amount of Ca^{2+} released from the control and that for LCA and CA, respectively.)

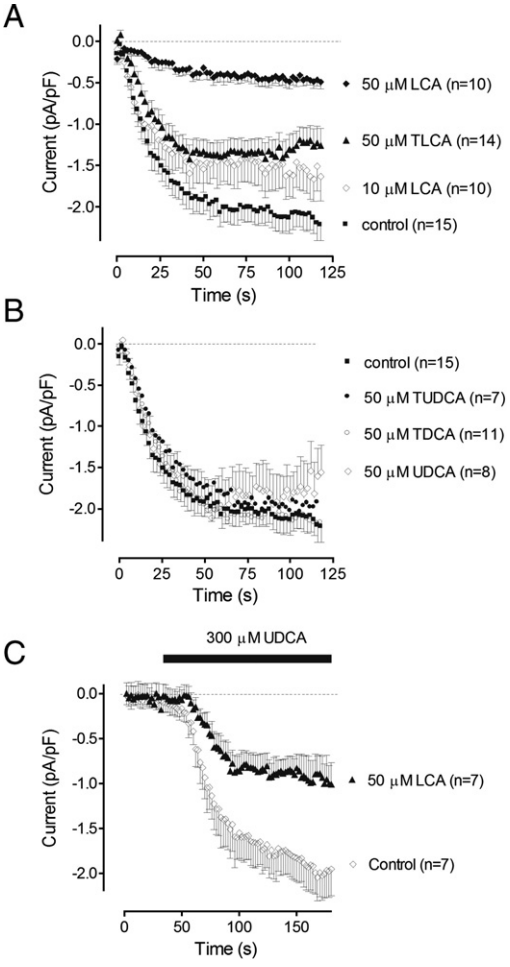

Fig. 6. Inhibition of I_{SOC} after pre-incubation of H4-IIE liver cells for 12 h with cholestatic bile acids. (A, B) Plots of IP_3-induced current as a function of time in H4-IIE cells pre-incubated with a given bile acid. (C) Plots of UDCA-induced current as a function of time in control cells and in cells pre-incubated with cholestatic bile acid LCA. H4-IIE cells were pre-incubated for 12 h with a given bile acid as described in Materials and methods. The amplitude of I_{SOC} activated by intracellular perfusion with IP_3 (20 μM in the patch pipette) was measured at −118 mV and plotted against time. The results are the means±SEM of the number of experiments indicated.

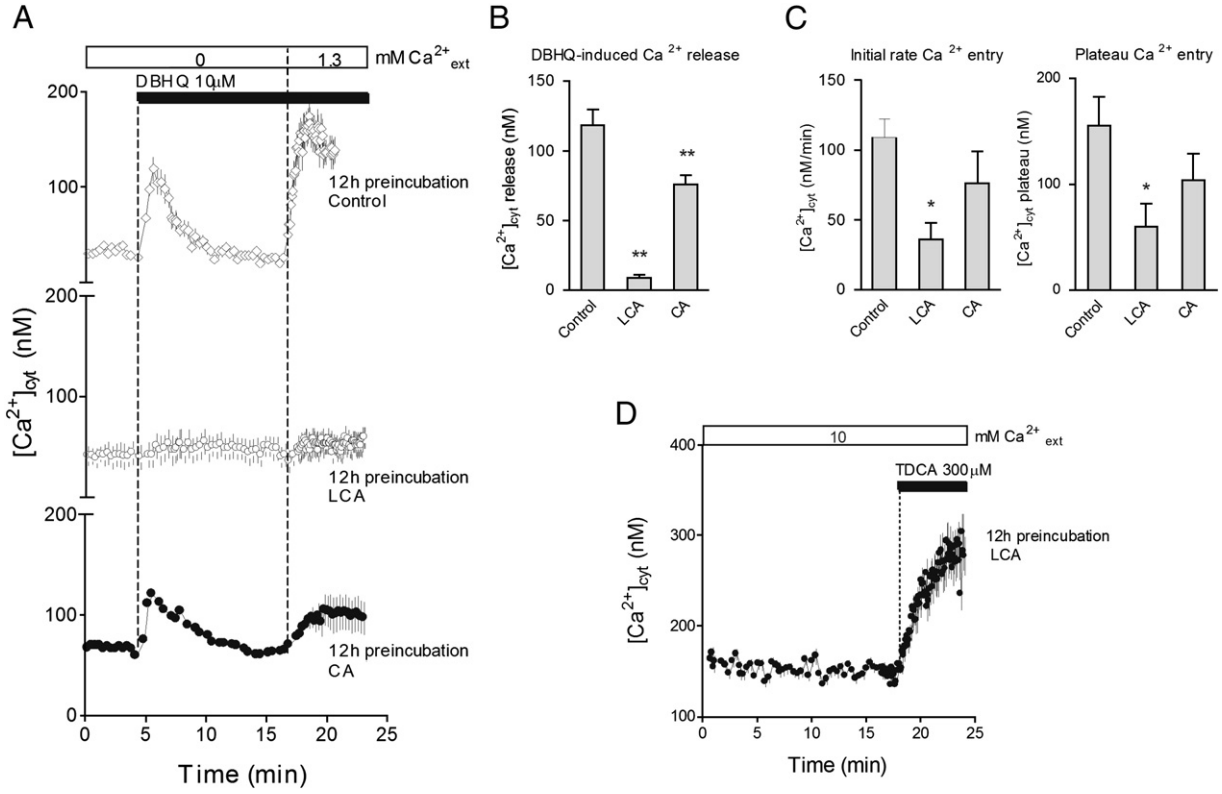

Fig. 7. Inhibition of DBHQ-stimulated Ca^{2+} entry after pre-incubation of H4-IIE liver cells for 12 h with the cholestatic bile acids LCA and CA. (A) Fura-2 loaded cells were exposed to the SERCA inhibitor DBHQ (10 μM) in the absence of Ca^{2+}_{ext}. When Ca^{2+} was added back to the bath the typical DBHQ-dependent increase in $[Ca^{2+}]_{cyt}$ was reduced in cells which were pre-treated for 12 h with 50 μM LCA or CA. (B) Amounts of Ca^{2+} released (peak height) by DBHQ in the presence and absence of LCA or CA. (C) Initial rates of Ca^{2+} entry and peak (plateau) values of $[Ca^{2+}]_{cyt}$ following Ca^{2+}_{ext} addition, determined as described in Materials and methods. (D) TDCA induces an increase in $[Ca^{2+}]_{cyt}$ in cells pre-incubated for 12 h with the cholestatic bile acid LCA. $[Ca^{2+}]_{cyt}$ was measured as a function of time in cells loaded with fura-2, as described in Materials and methods. (A, D) The additions to the bath are indicated by the horizontal bar. The results are representative of those obtained for one of 3 experiments which each gave similar results. (B, C) The values are the means±SEM of 6–7 experiments similar to the one shown in panel A. The degrees of significance between LCA and the control, and between CA and the control, determined using ANOVA followed by Bonferroni *post hoc* test, are $^{*}P<0.05$ and $^{**}P<0.01$.

3.3. Effects of bile acids on the intracellular distribution of STIM1

Since the redistribution of STIM1 in the ER and the localisation of some STIM1 at the plasma membrane are associated with the activation of SOCs in lymphocytes, mast cells, some other cell types [43–49], and liver cells [50], the effects of bile acids on STIM1 distribution in liver cells were investigated. In H4-IIE cells transfected with DNA encoding GFP-STIM1 and incubated in the absence of agonist (control cells), GFP fluorescence was distributed throughout the ER as indicated by co-localisation of GFP-STIM1 with the ER marker pDsRed2-ER (Fig. 8A). (Fig. 8A shows a confocal image of a cell in a *Z*-plane in the middle of the cell (the nucleus, which does not contain ER or STIM1 is evident).) TDCA caused a redistribution of GFP fluorescence to give a punctate pattern (Fig. 8B, TDCA) similar to that caused by thapsigargin (Fig. 8B, Tg). (Fig. 8B shows a confocal image of a cell in a *Z*-plane near the plasma membrane (no nucleus visible) and hence shows STIM1 distribution close to the plasma membrane.) When the distribution of endogenous STIM1 was monitored by immunofluorescence, it was also found that TDCA altered the distribution of STIM1 to give more concentrated localisations and a less dispersed pattern (Fig. 8C, TDCA). This was similar to that observed for the effects of thapsigargin (Fig. 8C, Tg). The effect of TDCA on STIM1 distribution was reversible (Fig. 8D).

Incubation of cells for 12 h with the cholestatic bile acid LCA also caused a redistribution of ectopically expressed GFP-STIM1 similar to that caused by thapsigargin (Fig. 8B, LCA). Incubation of cells with LCA (50 μM) for 5 min did not affect the distribution of STIM1, as monitored by GFP fluorescence in cells ectopically expressing GFP-STIM1 (results not shown).

To test the possibility that TDCA causes a re-organisation of the ER [56], cells were transfected with DNA encoding pDsRed2-ER. Neither TDCA (300 μM incubated for 15 min at 10 mM Ca^{2+}_{ext}) nor thapsigargin (1 μM incubated for 10 min in the absence of added Ca^{2+}_{ext}) caused any detectable change in the structure of the ER (results not shown). This indicates that the observed redistribution of STIM1 induced by TDCA and thapsigargin is unlikely to be due to a substantial rearrangement of ER structure. Pre-incubation of cells for 12 h with the cholestatic bile acid LCA (50 μM) also did not cause any detectable change in the structure of the ER (results not shown).

We have shown previously that knockdown of STIM1 in H4-IIE cells using siRNA inhibits development of the I_{SOC} in response to IP_3 or thapsigargin [50]. Here we investigated

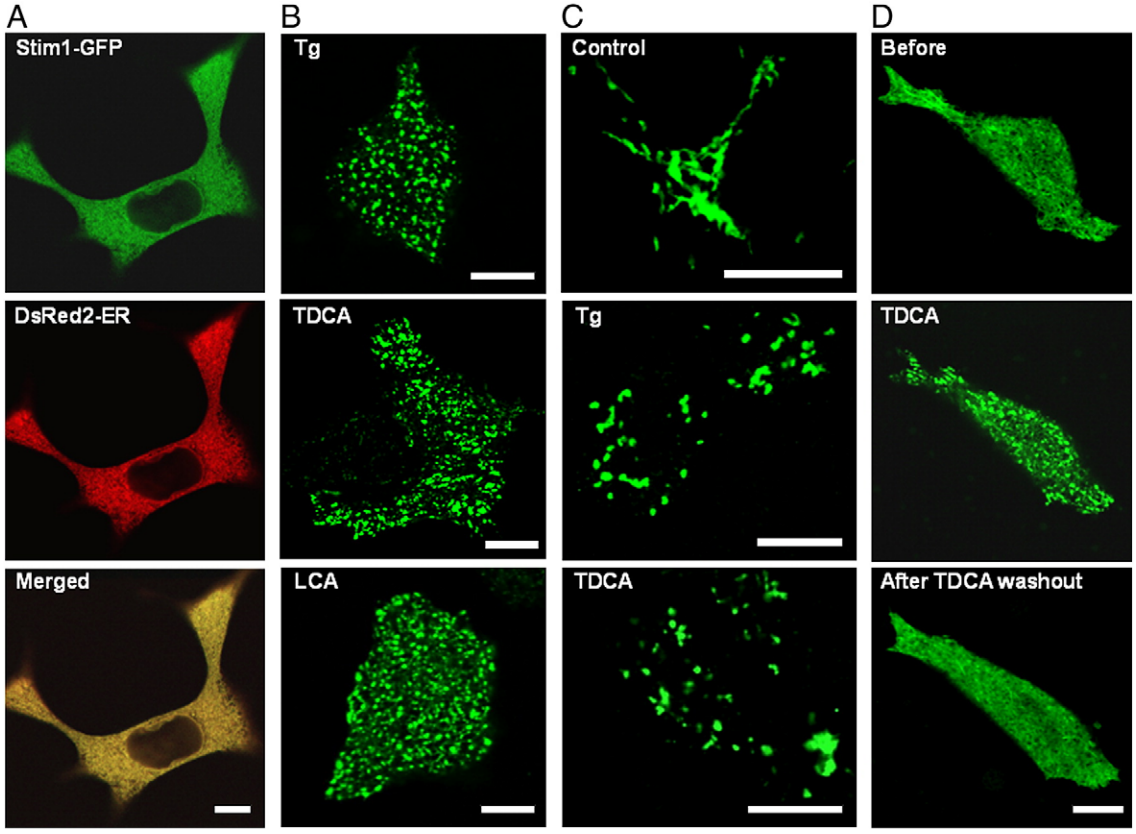

Fig. 8. Incubation of H4-IIE cells with choleretic TDCA or pre-incubation with cholestatic LCA causes a redistribution of STIM1. (A) Representative confocal images in a *Z*-plane in the middle (equatorial plane) of a cell co-expressing GFP-STIM1 and the ER marker psDsRed2-ER, and the merged image showing co-localisation of STIM1 and the ER. (B) Representative confocal images in a *Z*-plane close to the plasma membrane of GFP fluorescence in cells transfected with GFP-STIM1 and incubated with 1 μM thapsigargin for 10 min in the absence of added Ca^{2+}_{ext} (Tg); with 300 μM TDCA for 15 min at 10 mM Ca^{2+}_{ext} (TDCA); and with 50 μM LCA for 12 h at 1.3 mM Ca^{2+}_{ext} (LCA). (C) Representative confocal immunofluorescence images in a *Z*-plane close to the plasma membrane of endogenous STIM1 in cells incubated in the absence of agonist (Control), or in the presence of 1 μM thapsigargin for 10 min in the absence of added Ca^{2+}_{ext} (Tg), or with 300 μM TDCA for 10 min at 10 mM Ca^{2+}_{ext} (TDCA). (D) Representative confocal images in a *Z*-plane close to the plasma membrane of GFP fluorescence in a single cell transfected with GFP-STIM1 before addition of TDCA (Before), after TDCA addition (TDCA), and after washing out TDCA (After TDCA washout). The results are representative of those obtained for 18 cells in 4 separate experiments. Transfection of cells with DNA encoding GFP-STIM1, psDsRed2-ER, immunofluorescence, and confocal microscopy were conducted as described in Materials and methods. The images shown are representative of those obtained from at least 2 coverslips for each of 3 independent experiments conducted on different days. The scale bar represents 10 μm.

whether STIM1 is required for activation of I_{SOC} by choleretic bile salts. At 72 h post transfection with siRNA against STIM1 the amplitude of I_{SOC} activated by 300 μM UDCA was reduced by ~80% (Fig. 9A) and the initial rate of Ca^{2+} entry measured using fura-2 was inhibited by 50% (Fig. 9B). These results indicate that STIM1 is required for the activation of Ca^{2+} entry by choleretic bile acids.

4. Discussion

In this study with H4-IIE liver cells and rat hepatocytes we have shown that TDCA and other choleretic bile acids, when added directly to the bath, activate Ca^{2+} entry through the SOCs and cause a redistribution of STIM1 similar to the redistribution caused by thapsigargin. By contrast, LCA and other cholestatic bile acids, when pre-incubated with the cells for 12 h, inhibit Ca^{2+} entry through SOCs.

Evidence that the Ca^{2+} entry pathway activated by choleretic bile acids is the liver cell SOC is provided by the similarities between the current induced by choleretic bile acids and the current induced by IP_3 [34,36]. These include the Ca^{2+} selectivity, the time course of activation, the effects of substituting Ba^{2+} for Ca^{2+}, activation and inhibition by 2-APB, inhibition by La^{3+} and Gd^{3+}; and the observations that in the presence of IP_3, UDCA does not activate additional current and, in fura-2 loaded cells incubated in the presence of thapsigargin, TDCA does not further increase $[Ca^{2+}]_{cyt}$. Washout patch clamp and fura-2 experiments indicate that the ability of choleretic bile acid to activate Ca^{2+} entry is reversible. Several previous studies have shown that exposure of liver cells to choleretic bile acids induces an increase in $[Ca^{2+}]_{cyt}$ which subsequently affects diverse cellular process [7,26,57]. However the site(s) of action of the choleretic bile acids on cellular Ca^{2+} movements was not clearly defined. Our results identify SOCs as a target for choleretic bile acids in liver cells. While TDCA induced a sustained increase in $[Ca^{2+}]_{cyt}$, TUDCA induced oscillations in $[Ca^{2+}]_{cyt}$. These differences may relate to the degree of involvement of ryanodine receptors in the bile acid Ca^{2+} response [58].

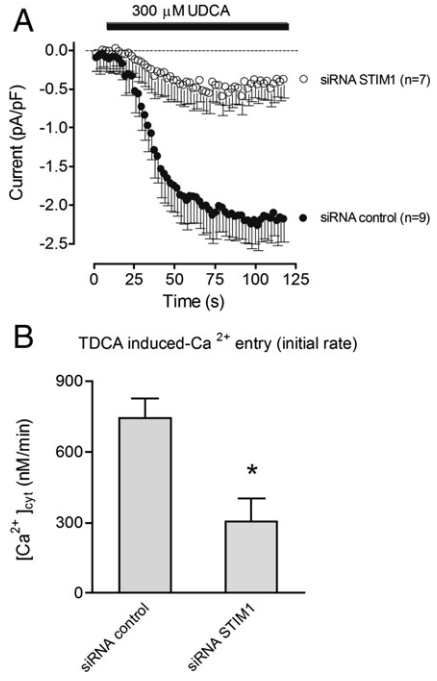

Fig. 9. Knockdown of STIM1 expression using siRNA causes a substantial reduction in UDCA-induced Ca^{2+} entry. (A) Inward currents measured at −118 mV in the presence of UDCA (indicated by the horizontal bar) plotted as a function of time for cells treated with siRNA directed against STIM1 and control siRNA. The results are the means±SEM of the number of experiments indicated. (B) Initial rates of Ca^{2+} entry measured in cells loaded with fura-2 using the Ca^{2+} add-back assay. The results in (B) are the means±SEM of 3 experiments. The degree of significance, determined using Student's *t*-test for unpaired samples is $*P<0.05$.

Results obtained with GFP-STIM1, immunofluorescence and fluorescence microscopy indicate that the activation of Ca^{2+} entry through SOCs by TDCA is associated with a redistribution of STIM1 similar to that caused by the SERCA inhibitor thapsigargin. The redistribution of STIM1 by TDCA was reversible, indicating that TDCA does not act by inducing the covalent modification of a protein, or as a tight-binding inhibitor, and is unlikely to cause non-specific damage to the plasma membrane or to intracellular membranes. Since TDCA caused a redistribution of STIM1 similar to that caused by thapsigargin, it is considered most likely that the mechanism by which TDCA activates SOCs involves the release of Ca^{2+} from ER, the movement and relocalisation of STIM1, and the activation of SOCs by STIM1 through the interaction of STIM1 with a member of the Orai family (reviewed in [41]) (shown schematically in Fig. 10A).

The pre-incubation of liver cells with a cholestatic bile acid resulted in inhibition of Ca^{2+} entry through SOCs and no detectable release of Ca^{2+} from intracellular stores when DBHQ was subsequently added. The latter result suggests that either the intracellular Ca^{2+} stores were depleted of Ca^{2+} before DBHQ addition, or that the interaction of cholestatic bile acids with the ER leads to disruption of the action of DBHQ on SERCAs. While the amount of Ca^{2+} in intracellular stores was not directly measured, it is considered that the most likely explanation is that pre-incubation with LCA induces Ca^{2+} release from intracellular stores. This is consistent with previous findings that cholestatic bile acids inhibit SERCA pumps leading to Ca^{2+} depletion of the ER [59,60].

Since the release of Ca^{2+} from the ER and a redistribution of STIM1 are pre-requisites for the activation of SOCs (reviewed in [41]), it might be expected that, if pre-incubation with cholestatic bile acids leads to depletion of the ER Ca^{2+} stores and redistribution of STIM1, SOCs would be constitutively activated (i.e. active in the absence of IP_3 or SERCA inhibitor). Hence, it is, perhaps, surprising that the release of Ca^{2+} from intracellular stores and redistribution of STIM1 induced by pre-incubation with cholestatic bile acids are associated with inhibition of Ca^{2+}

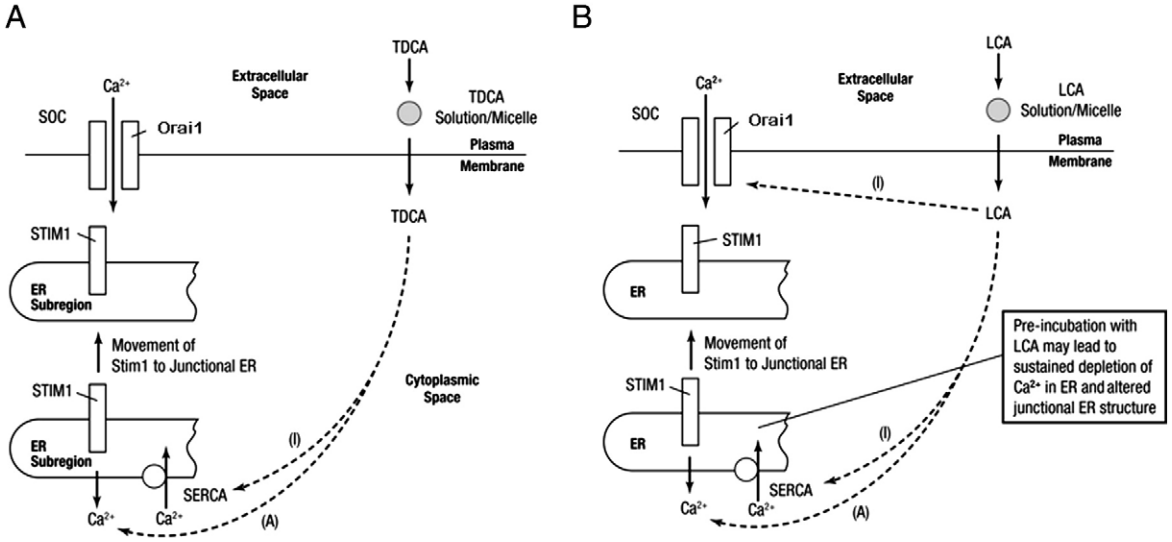

Fig. 10. A schematic representation of the proposed mechanisms by which choleretic TDCA activates SOCs (A) and cholestatic LCA inhibits SOCs (B) in hepatocytes. Activation (A) and inhibition (I) are indicated by the broken lines. (A) It is proposed that TDCA induces the release of Ca^{2+} from the ER by enhancing Ca^{2+} outflow [26,28,29] or by inhibiting SERCA [59,60]. This, in turn, leads to the movement of STIM1 to the junctional ER close to the plasma membrane and the subsequent activation of SOCs. (B) It is proposed that pre-incubation with LCA causes a sustained release of Ca^{2+} from the ER, which in turn leads to relocalisation of STIM1, an alteration in the fine structure of the junctional ER and/or inhibition of movement of Orai1 in the plasma membrane so there is no activation of SOCs.

entry. Moreover, this inhibition could be partially counteracted by a choleretic bile acid. It is clear that this can only occur if the effects of bile acids are not restricted to the depletion of Ca^{2+} stores alone. There must be some other component(s) of store-operated Ca^{2+} entry that is affected by cholestatic and choleretic bile acids in opposite ways. One possible explanation is that cholestatic bile acids inhibit, while choleretic bile acids facilitate, a step in the pathway of activation of SOCs downstream from the release of Ca^{2+} from the ER and redistribution of STIM1 [61]. Cholestatic and choleretic bile acids might have differential effects on the movement of Orai1 in the plasma membrane towards junctional ER sites, the interaction between STIM1 and Orai1, or the open probability of Orai1. It has been shown previously that impairment of hepatobiliary exocytosis and bile flow caused by TLCA is associated with activation of phosphatidylinositol 3-kinase and the translocation of protein kinase Cε to the plasma membrane [62]. At the same time it was also shown that TUDCA inhibits the activity of phosphatidylinositol 3-kinase-dependant protein kinase B and membrane binding of protein kinase Cε, thus reversing the effects of TLCA [62]. It is possible that differential regulation of protein kinase Cε and phosphatidylinositol 3-kinase by TUDCA and TLCA underlies their opposite effects on Ca^{2+} entry through SOCs. However, this is yet to be investigated. The possible pathways of action of the cholestatic bile acid LCA are shown schematically in Fig. 10B.

The results reported here may have implications for understanding the progression of cholestasis and subsequent damage to hepatocytes, and for the treatment of cholestasis. Previous studies have provided some evidence that Ca^{2+} entry through SOCs is required for normal bile flow, most likely by contributing to the increase in $[Ca^{2+}]_{cyt}$ which initiates contraction of the bile canaliculus [38]. The inhibition of Ca^{2+} entry through SOCs by cholestatic bile acids would lead to the disruption of intracellular Ca^{2+} homeostasis and downstream Ca^{2+} signaling pathways. This may contribute to the further inhibition of bile flow, and altered hepatocyte growth, apoptosis and necrosis which are consequences of cholestasis [7–12].

The choleretic bile acids UDCA and TUDCA are used pharmacologically to enhance bile flow in cholestatic conditions [13–23,63], and for the treatment of liver dysfunction in patients with acute and chronic intrahepatic cholestatic disorders [17,64], primary biliary cirrhosis [18,19] and primary sclerosing cholangitis [20]. Moreover, it has been shown in rat models of cholestasis, that treatment with choleretic bile acids can stimulate bile flow [65]. The present results, showing that choleretic bile acids activate Ca^{2+} entry through SOCs, and can activate Ca^{2+} entry in cells previously treated for 12 h with a cholestatic bile acid, may provide a mechanism by which choleretic bile acids exert beneficial effects on cholestasis.

It is concluded that SOCs and STIM1 are important targets for the actions of bile acids on hepatocytes. Inhibition of Ca^{2+} entry through SOCs by cholestatic bile acids may be responsible for enhancing the cholestatic condition, and activation of Ca^{2+} entry through SOCs may contribute to explaining the beneficial pharmacological effects of choleretic bile acids.

Acknowledgements

We would like to thank Rachael Hughes and Yabin Zhou for preparing isolated rat hepatocytes, Dr T Kurosaki, RIKEN Research Centre for Allergy and Immunology, Kanagwa, Japan, for providing the GFP-STIM1 plasmid, Dr Mike Schell, USUHS, Bethesda for advice on cell transfections, and Dr Alan F Hofmann, University of California, for discussions on bile acid solubility. This work was supported by the Australian Research Council and the National Health and Medical Research Council of Australia and the Flinders Medical Centre Foundation.

References

[1] J.G. O'Leary, D.S. Pratt, Cholestasis and cholestatic syndromes, Curr. Opin. Gastroenterol. 23 (2007) 232–236.
[2] J.L. Boyer, Schiffs Diseases of the Liver, Lippincott, Williams & Wilkins, Philadelphia, 2002, pp. 135–165.
[3] W.C. Maddrey, Schiffs Diseases of the Liver, Lippincott, Williams & Wilkins, Philadelphia, 2002, pp. 647–649.
[4] J.L. Boyer, Molecular pathophysiology of membrane transport function in cholestasis, The Liver: Biology and Pathobiology, 2001, pp. 663–677.
[5] N.B. Javitt, Cholestasis in rats induced by taurolithocholate, Nature 210 (1966) 1262–1263.
[6] N.B. Javitt, S. Emerman, Effect of sodium taurolithocholate on bile flow and bile acid excretion, J. Clin. Invest. 47 (1968) 1002–1014.
[7] M. Borgognone, L.M. Perez, C.L. Basiglio, J.E. Ochoa, M.G. Roma, Signaling modulation of bile salt-induced necrosis in isolated rat hepatocytes, Toxicol. Sci. 83 (2005) 114–125.
[8] P. Chieco, E. Romagnoli, G. Aicardi, A. Suozzi, G.C. Forti, A. Roda, Apoptosis induced in rat hepatocytes by in vivo exposure to taurochenodeoxycholate, Histochem. J. 29 (1997) 875–883.
[9] C. Benz, S. Angermuller, U. Tox, P. Kloters-Plachky, H.D. Riedel, P. Sauer, W. Stremmel, A. Stiehl, Effect of tauroursodeoxycholic acid on bile-acid-induced apoptosis and cytolysis in rat hepatocytes, J. Hepatol. 28 (1998) 99–106.
[10] H. Higuchi, G.J. Gores, Bile acid regulation of hepatic physiology: IV. Bile acids and death receptors, Amer. J. Physiol. Gastroint. Liver Physiol. 284 (2003) G734–G738.
[11] H. Higuchi, J.H. Yoon, A. Grambihler, N. Werneburg, S.F. Bronk, G.J. Gores, Bile acids stimulate cFLIP phosphorylation enhancing TRAIL-mediated apoptosis, J. Biol. Chem. 278 (2003) 454–461.
[12] T. Sodeman, S.F. Bronk, P.J. Roberts, H. Miyoshi, G.J. Gores, Bile salts mediate hepatocyte apoptosis by increasing cell surface trafficking of Fas, Amer. J. Physiol. Gastroint. Liver Physiol. 278 (2000) G992–G999.
[13] S. Kinbara, K. Ishizaki, H. Sakakura, N. Hirabayashi, H. Kasai, T. Araki, Improvement of estradiol-17 beta-D-glucuronide-induced cholestasis by sodium tauroursodeoxycholate therapy in rats, Scandinavian J. Gastroent. 32 (1997) 947–952.
[14] S.A. Azer, P.J. Canfield, N.H. Stacey, Hepatoprotection in ethinylestradiol-treated rats is provided by tauroursodeoxycholic acid, but not by ursodeoxycholic acid, J. Gastroent. Hepatol. 10 (1995) 261–269.
[15] G. Bouchard, I.M. Yousef, B. Tuchweber, Influence of oral treatment with ursodeoxycholic and tauroursodeoxycholic acids on estrogen-induced cholestasis in rats: effects on bile formation and liver plasma membranes, Liver 13 (1993) 193–202.
[16] E. Jacquemin, M. Dumont, A. Mallet, S. Erlinger, Ursodeoxycholic acid improves ethinyl estradiol-induced cholestasis in the rat, European J. Clin. Invest. 23 (1993) 794–802.
[17] P. Fabris, G. Tositti, G. Mazzella, A.R. Zanetti, R. Nicolin, G. Pellizzer, P. Benedetti, F. de Lalla, Effect of ursodeoxycholic acid administration in patients with acute viral hepatitis: a pilot study, Aliment. Pharmacol. Ther. 13 (1999) 1187–1193.
[18] A. Pares, L. Caballeria, J. Rodes, M. Bruguera, L. Rodrigo, A. Garcia-Plaza, J. Berenguer, D. Rodriguez-Martinez, J. Mercader, R. Velicia, UDCA-Cooperative Group from the Spanish Association for the Study of the Liver,

Long-term effects of ursodeoxycholic acid in primary biliary cirrhosis: results of a double-blind controlled multicentric trial, J. Hepatol. 32 (2000) 561–566.
[19] R.E. Poupon, K.D. Lindor, K. Cauch-Dudek, E.R. Dickson, R. Poupon, E.J. Heathcote, Combined analysis of randomized controlled trials of ursodeoxycholic acid in primary biliary cirrhosis, Gastroenterology 113 (1997) 884–890.
[20] P.C. van de Meeberg, F.H. Wolfhagen, G.P. Van Berge-Henegouwen, J.M. Salemans, A. Tangerman, H.R. van Buuren, J. van Hattum, K.J. van Erpecum, Single or multiple dose ursodeoxycholic acid for cholestatic liver disease: biliary enrichment and biochemical response, J. Hepatol. 25 (1996) 887–894.
[21] K.N. Lazaridis, G.J. Gores, K.D. Lindor, Ursodeoxycholic acid 'mechanisms of action and clinical use in hepatobiliary disorders', J. Hepatol. 35 (2001) 134–146.
[22] U. Beuers, J.L. Boyer, G. Paumgartner, Ursodeoxycholic acid in cholestasis: potential mechanisms of action and therapeutic applications, Hepatology 28 (1998) 1449–1453.
[23] T. Ono, K. Imai, H. Kohno, M. Uchida, Y. Takemoto, D.K. Dhar, N. Nagasue, Tauroursodeoxycholic acid protects cholestasis in rat reperfused livers: its roles in hepatic calcium mobilization, Dig. Dis. Sci. 43 (1998) 2201–2210.
[24] U. Beuers, I. Probst, C. Soroka, J.L. Boyer, G.A. Kullak-Ublick, G. Paumgartner, Modulation of protein kinase C by taurolithocholic acid in isolated rat hepatocytes, Hepatology 29 (1999) 477–482.
[25] L. Combettes, B. Berthon, E. Doucet, S. Erlinger, M. Claret, Bile acids mobilise internal Ca^{2+} independently of external Ca^{2+} in rat hepatocytes, Eur. J. Biochem. 190 (1990) 619–623.
[26] U. Beuers, M.H. Nathanson, J.L. Boyer, Effects of tauroursodeoxycholic acid on cytosolic Ca^{2+} signals in isolated rat hepatocytes, Gastroenterology 104 (1993) 604–612.
[27] B. Bouscarel, H. Fromm, R. Nussbaum, Ursodeoxycholate mobilizes intracellular Ca^{2+} and activates phosphorylase a in isolated hepatocytes, Amer. J. Physiol. 264 (1993) G243–G251.
[28] L. Combettes, M. Dumont, B. Berthon, S. Erlinger, M. Claret, Effect of the bile acid taurolithocholate on cell calcium in saponin-treated rat hepatocytes, FEBS Letters 227 (1988) 161–166.
[29] L. Combettes, M. Dumont, B. Berthon, S. Erlinger, M. Claret, Release of calcium from the endoplasmic reticulum by bile acids in rat liver cells, J. Biol. Chem. 263 (1988) 2299–2303.
[30] U. Beuers, M.H. Nathanson, C.M. Isales, J.L. Boyer, Tauroursodeoxycholic acid stimulates hepatocellular exocytosis and mobilizes extracellular Ca^{++} mechanisms defective in cholestasis, J. Clin. Invest. 92 (1993) 2984–2993.
[31] S. Watanabe, M.J. Phillips, Ca^{2+} causes active contraction of bile canaliculi: direct evidence from microinjection studies, Proc. Natl. Acad. Sci. U. S. A. 81 (1984) 6164–6168.
[32] J.V. Gerasimenko, S.E. Flowerdew, S.G. Voronina, T.K. Sukhomlin, A.V. Tepikin, O.H. Petersen, O.V. Gerasimenko, Bile acids induce Ca^{2+} release from both the endoplasmic reticulum and acidic intracellular calcium stores through activation of inositol trisphosphate receptors and ryanodine receptors, J. Biol. Chem. 281 (2006) 40154–40163.
[33] G. Rychkov, H.M. Brereton, M.L. Harland, G.J. Barritt, Plasma membrane Ca^{2+} release-activated Ca^{2+} channels with a high selectivity for Ca^{2+} identified by patch-clamp recording in rat liver cells, Hepatology 33 (2001) 938–947.
[34] G.Y. Rychkov, T. Litjens, M.L. Roberts, G.J. Barritt, ATP and vasopressin activate a single type of store-operated Ca^{2+} channel, identified by patch-clamp recording, in rat hepatocytes, Cell Calcium 37 (2005) 183–191.
[35] E.C. Aromataris, M.L. Roberts, G.J. Barritt, G.Y. Rychkov, Glucagon activates Ca^{2+} and Cl^- channels in rat hepatocytes, J. Physiol. 573 (2006) 611–625.
[36] T. Litjens, M.L. Harland, M.L. Roberts, G.J. Barritt, G.Y. Rychkov, Fast Ca(2+)-dependent inactivation of the store-operated Ca^{2+} current (I_{SOC}) in liver cells: a role for calmodulin, J. Physiol. 558 (2004) 85–97.
[37] G.J. Barritt, in: R. Pochet, R. Donato, J. Haiech, C.W. Heizmann, V. Gerke (Eds.), Calcium: the Molecular Basis of Calcium Action in Biology and Medicine, Kluwer Academic Publishers, 2000, pp. 73–94.
[38] R.B. Gregory, R. Hughes, G.J. Barritt, Induction of cholestasis in the perfused rat liver by 2-aminoethyl diphenylborate, an inhibitor of the hepatocyte plasma membrane Ca^{2+} channels, J. Gastroent. Hepatol. 19 (2004) 1128–1134.
[39] A.B. Parekh, J.W. Putney Jr., Store-operated calcium channels, Physiol. Rev. 85 (2005) 757–810.
[40] W.I. Dehaven, J.T. Smyth, R.R. Boyles, J.W. Putney Jr., Calcium inhibition and calcium potentiation of orai1, orai2 and orai3 calcium-release-activated calcium channels, J. Biol. Chem. (2007).
[41] R.S. Lewis, The molecular choreography of a store-operated calcium channel, Nature 446 (2007) 284–287.
[42] C.W. Taylor, Store-operated Ca2+ entry: a STIMulating stOrai, Trends in Biochem. Sci. 31 (2006) 597–601.
[43] Y. Baba, K. Hayashi, Y. Fujii, A. Mizushima, H. Watarai, M. Wakamori, T. Numaga, Y. Mori, M. Iino, M. Hikida, T. Kurosaki, Coupling of STIM1 to store-operated Ca^{2+} entry through its constitutive and inducible movement in the endoplasmic reticulum, Proc. Natl. Acad. Sci. U. S. A. 103 (2006) 16704–16709.
[44] J. Liou, M.L. Kim, W.D. Heo, J.T. Jones, J.W. Myers, J.E. Ferrell Jr., T. Meyer, STIM is a Ca^{2+} sensor essential for Ca^{2+}-store-depletion-triggered Ca^{2+} influx, Curr. Biol. 15 (2005) 1235–1241.
[45] J.C. Mercer, W.I. Dehaven, J.T. Smyth, B. Wedel, R.R. Boyles, G.S. Bird, J.W. Putney Jr., Large store-operated calcium selective currents due to co-expression of Orai1 or Orai2 with the intracellular calcium sensor, Stim1, J. Biol. Chem. 281 (2006) 24979–24990.
[46] H.L. Ong, X. Liu, K. Tsaneva-Atanasova, B.B. Singh, B.C. Bandyopadhyay, W.D. Swaim, J.T. Russell, R.S. Hegde, A. Sherman, I.S. Ambudkar, Relocalization of stim1 for activation of store-operated Ca^{2+} entry is determined by the depletion of subplasma membrane endoplasmic reticulum Ca^{2+} store, J. Biol. Chem. 282 (2007) 12176–12185.
[47] M.M. Wu, J. Buchanan, R.M. Luik, R.S. Lewis, Ca^{2+} store depletion causes STIM1 to accumulate in ER regions closely associated with the plasma membrane, J. Cell Biol. 174 (2006) 803–813.
[48] P. Xu, J. Lu, Z. Li, X. Yu, L. Chen, T. Xu, Aggregation of STIM1 underneath the plasma membrane induces clustering of Orai1, Biochem. Biophys. Res. Comm. 350 (2006) 969–976.
[49] J. Liou, M. Fivaz, T. Inoue, T. Meyer, Live-cell imaging reveals sequential oligomerization and local plasma membrane targeting of stromal interaction molecule 1 after Ca^{2+} store depletion, Proc. Natl. Acad. Sci. U. S. A. 104 (2007) 9301–9306.
[50] T. Litjens, T. Nguyen, J. Castro, E.C. Aromataris, L. Jones, G.J. Barritt, G.Y. Rychkov, Phospholipase C-gamma1 is required for the activation of store-operated Ca2+ channels in liver cells, Biochem. J. 405 (2007) 269–276.
[51] G.J. Darlington, Liver cell lines, Methods Enzymol. 151 (1987) 19–38.
[52] P.H. Barry, JPCalc, a software package for calculating liquid junction potential corrections in patch–clamp, intracellular, epithelial and bilayer measurements and for correcting junction potential measurements, J. Neurosci. Methods 51 (1994) 107–116.
[53] G. Grynkiewicz, M. Poenie, R.Y. Tsien, A new generation of Ca^{2+} indicators with greatly improved fluorescence properties, J. Biol. Chem. 260 (1985) 3440–3450.
[54] J.J. Gu, A.F. Hofmann, H.T. Ton-Nu, C.D. Schteingart, K.J. Mysels, Solubility of calcium salts of unconjugated and conjugated natural bile acids, J. Lipid Res. 33 (1992) 635–646.
[55] A.F. Hofmann, K.J. Mysels, Bile acid solubility and precipitation in vitro and in vivo: the role of conjugation, pH, and Ca^{2+} ions, J. Lipid Res. 33 (1992) 617–626.
[56] C.M. Payne, C.L. Crowley-Weber, K. Dvorak, C. Bernstein, H. Bernstein, H. Holubec, C. Crowley, H. Garewal, Mitochondrial perturbation attenuates bile acid-induced cytotoxicity, Cell Biol. Toxicol. 21 (2005) 215–231.
[57] G. Alpini, N. Kanno, J.L. Phinizy, S. Glaser, H. Francis, S. Taffetani, G. LeSage, Tauroursodeoxycholate inhibits human cholangiocarcinoma growth via Ca^{2+}-, PKC-, and MAPK-dependent pathways, Amer. J. Physiol. Gastroint. Liver Physiol. 286 (2004) G973–G982.
[58] I. Marrero, A. Sanchez-Bueno, P.H. Cobbold, C.J. Dixon, Taurolithocholate and taurolithocholate 3-sulphate exert different effects on cytosolic free Ca^{2+} concentration in rat hepatocytes, Biochem. J. 300 (1994) 383–386.

[59] J.Y. Kim, K.H. Kim, J.A. Lee, W. Namkung, A.Q. Sun, M. Ananthanarayanan, F.J. Suchy, D.M. Shin, S. Muallem, M.G. Lee, Transporter-mediated bile acid uptake causes Ca^{2+}-dependent cell death in rat pancreatic acinar cells [see comment], Gastroenterology 122 (2002) 1941–1953.
[60] B.W. Lau, M. Colella, W.C. Ruder, M. Ranieri, S. Curci, A.M. Hofer, Deoxycholic acid activates protein kinase C and phospholipase C via increased Ca^{2+} entry at plasma membrane, Gastroenterology 128 (2005) 695–707.
[61] P. Varnai, B. Toth, D.J. Toth, L. Hunyady, T. Balla, Visualization and manipulation of plasma membrane-endoplasmic reticulum contact sites indicates the presence of additional molecular components within the STIM1–Orai1 complex, J. Biol. Chem. 282 (2007) 29678–29690.
[62] U. Beuers, G.U. Denk, C.J. Soroka, R. Wimmer, C. Rust, G. Paumgartner, J.L. Boyer, Taurolithocholic acid exerts cholestatic effects via phosphatidylinositol 3-kinase-dependent mechanisms in perfused rat livers and rat hepatocyte couplets, J. Biol. Chem. 278 (2003) 17810–17818.
[63] K. Tsukahara, S. Kanai, M. Ohta, K. Kitani, Taurine conjugate of ursodeoxycholate plays a major role in the hepatoprotective effect against cholestasis induced by taurochenodeoxycholate in rats, Liver 13 (1993) 262–269.
[64] S. Friman, J. Svanvik, A possible role of ursodeoxycholic acid in liver transplantation, Scandinavian J. Gastroent. Suppl. 204 (1994) 62–64.
[65] K. Ishizaki, S. Kinbara, N. Hirabayashi, K. Uchiyama, M. Maeda, Effect of sodium tauroursodeoxycholate on phalloidin-induced cholestasis in rats, Eur. J. Pharmacol. 421 (2001) 55–60.